

$(\pi, 0)$ antiferromagnetic spin excitations in superconducting $\text{Rb}_{0.82}\text{Fe}_{1.68}\text{Se}_2$

Miaoyin Wang,¹ Chunhong Li,² D. L. Abernathy,³ Yu Song,¹ Scott V. Carr,¹
Xingye Lu,^{2,1} Shiliang Li,² Jiangping Hu,^{4,2} Tao Xiang,² and Pengcheng Dai^{1,2,*}

¹*Department of Physics and Astronomy, The University of Tennessee, Knoxville, Tennessee 37996-1200, USA*

²*Beijing National Laboratory for Condensed Matter Physics and Institute of Physics,
Chinese Academy of Sciences, P. O. Box 603, Beijing 100190, China*

³*Neutron Scattering Science Division, Oak Ridge National Laboratory, Oak Ridge, Tennessee 37831-6393, USA*

⁴*Department of Physics, Purdue University, West Lafayette, Indiana 47907, USA*

We use inelastic neutron scattering to show that superconducting (SC) rubidium iron selenide $\text{Rb}_{0.82}\text{Fe}_{1.68}\text{Se}_2$ exhibits antiferromagnetic (AF) spin excitations near the in-plane wave vector $Q = (\pi, 0)$ identical to that for iron arsenide superconductors. Moreover, we find that these excitations change from incommensurate to commensurate with increasing energy, and occur at the expense of spin waves associated with the coexisting $\sqrt{5} \times \sqrt{5}$ block AF phase. Since angle resolved photoemission experiments reveal no evidence for hole-like Fermi surface at $\Gamma(0, 0)$, our results suggest that the $Q = (\pi, 0)$ excitations in SC $\text{Rb}_{0.82}\text{Fe}_{1.68}\text{Se}_2$ come from localized moments and may have a similar origin as the hourglass-like spin excitations in copper oxide superconductors.

Introduction The family of alkaline iron selenide superconductors $A_y\text{Fe}_{1.6+x}\text{Se}_2$ ($A = \text{K}, \text{Rb}, \text{Cs}$) [1–4] has generated considerable interest because superconductivity in these materials may have a different origin from the sign reversed s -wave electron pairing mechanism [5–7], a leading candidate for superconductivity in iron pnictide superconductors [8]. Although $A_y\text{Fe}_{1.6+x}\text{Se}_2$ materials are isostructural with the metallic iron pnictides such as $(\text{Ba}, \text{Ca}, \text{Sr})\text{Fe}_2\text{As}_2$ [9], they are insulators near $x = 0$ [3, 4] and form a $\sqrt{5} \times \sqrt{5}$ block AF structure with Fe vacancy order (Fig. 1a) [10–14] completely different from the collinear AF structure of the iron pnictides [15]. Since superconductivity in $A_y\text{Fe}_{1.6+x}\text{Se}_2$ always appears concurrently with the block AF order [11–14], whereas in the iron pnictides superconductivity arises at the expense of the static AF order [15], it is important to determine the relationship between superconductivity and magnetism in these materials. Although experiments using transmission electron microscopy [16], X-ray diffraction [17], muon-spin rotation (μSR) [18], scanning tunneling microscopy [19], angle resolved photoemission (ARPES) [20], Mössbauer [21], and optical [22, 23] spectroscopy have provided tantalizing evidence for several coexisting phases in superconducting (SC) $A\text{Fe}_{1.6+x}\text{Se}_2$, it is still unclear what is the exact crystal structure and stoichiometry of the SC phase and its relationship to the $\sqrt{5} \times \sqrt{5}$ AF phase.

For iron pnictides [9], band structure calculations have predicted that Fermi surfaces of these materials are composed of hole and electron pockets near $\Gamma(0, 0)$ and $M(\pi, 0)/M(0, \pi)$ points, respectively [8]. Since antiferromagnetism and superconductivity can arise from the sign reversed quasiparticle excitations between the hole and electron pockets [8], there should be a neutron spin resonance at the in-plane wave vector $Q = (\pi, 0)$ [24, 25]. Indeed, inelastic neutron scattering experiments on single crystals of electron and hole-doped BaFe_2As_2 have found the resonance at $Q = (\pi, 0)$ [26–29] and thus provided evidence for the electron s^\pm -wave pairing mechanism [8]. In the case of SC $A_y\text{Fe}_{1.6+x}\text{Se}_2$, since ARPES measurements [5–7] found electron Fermi surfaces at the $M(\pi, 0)/M(0, \pi)$ points but no hole Fermi surface near $\Gamma(0, 0)$, quasiparticle excitations between $\Gamma(0, 0)$ and $M(\pi, 0)/M(0, \pi)$ should not provide AF spin excitations at $Q = (\pi, 0)$ (Fig. 1c). Instead, the nesting properties between the $M(\pi, 0)/M(0, \pi)$ electron pockets in a d -wave symmetry is expected to give a broad plateau like maximum around $Q = (\pi, \pi)$ that is bordered by two peaks at $Q \approx (\pi, 0.625\pi)$ and $Q \approx (0.625\pi, \pi)$ [30]. Although the recent discovery of the neutron spin resonance in SC $\text{Rb}_y\text{Fe}_{1.6+x}\text{Se}_2$ at wave vectors $Q = (\pm\pi, \pm 0.5\pi)$ [or $Q = (\pm 0.5\pi, \pm\pi)$] (Fig. 1d) [31, 32] is consistent with this picture [30], it remains unknown whether there are spin excitations at other wave vectors not associated with the Fermi surface nesting.

In this Letter, we use neutron scattering to map out the low-energy spin excitations in SC $\text{Rb}_{0.82}\text{Fe}_{1.68}\text{Se}_2$ ($T_c = 32$ K, Fig. 1f). In addition to confirming the neutron spin resonance at $Q = (\pm\pi, \pm 0.5\pi)$ [31, 32], we find clear evidence for incommensurate spin excitations near wave vector $Q = (\pi, 0)$ that are absent in insulating $\text{Rb}_{0.89}\text{Fe}_{1.58}\text{Se}_2$ (Figs. 1b and 1d) [33]. With increasing energy, the incommensurate spin excitations disperse inward to $Q = (\pi, 0)$ and disappear above $E = 30$ meV (Figs. 2, 3). A comparison of spin excitations in SC $\text{Rb}_{0.82}\text{Fe}_{1.68}\text{Se}_2$ with spin waves in insulating $\text{Rb}_{0.89}\text{Fe}_{1.58}\text{Se}_2$ [33] reveals that the intensity gain of the $Q = (\pi, 0)$ excitations is at the expense of spin waves associated with the $\sqrt{5} \times \sqrt{5}$ AF phase (Fig. 3). Since electron-hole pocket excitations are impossible between $\Gamma(0, 0)$ and $M(\pi, 0)/M(0, \pi)$ points [5–7], our results suggest the presence of local moments [34] in addition to the itinerant electron induced resonance [31, 32]. Moreover, the dispersion of the $Q = (\pi, 0)$ excitations is similar to that of copper oxide superconductors [35, 36] and insulating cobalt oxide [37], thus suggesting the possible presence of dynamic stripes [38].

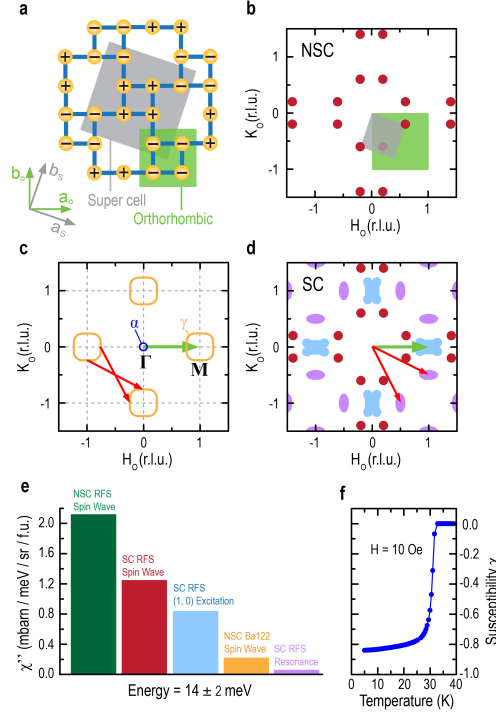


FIG. 1: (Color online) (a) The block antiferromagnetic spin structure of the insulating $A_y\text{Fe}_{1.6+x}\text{Se}_2$, where the $\sqrt{5} \times \sqrt{5}$ superlattice structure is marked as grey with lattice parameter $a_s = 8.663 \text{ \AA}$ and the orthorhombic lattice cell similar to iron pnictides is shaded green [33]. (b) The reciprocal space in the $[H_o, K_o]$ plane, where the solid red circles indicate the AF Bragg peak positions. (c) Schematics of the Fermi surfaces of SC $A_y\text{Fe}_{1.6+x}\text{Se}_2$ from ARPES measurements. There are four large electron pockets at $Q = (\pm 1, 0)/(0, \pm 1)$ and a small electron pocket at $\Gamma(0, 0)$ [5–7]. The neutron spin resonance is believed to originate from the electron-electron pocket excitations as shown by the red arrows [31, 32]. The green arrow indicates the $\Gamma \leftrightarrow M$ transition. (d) Positions of observed spin excitations in SC $\text{Rb}_{0.82}\text{Fe}_{1.68}\text{Se}_2$, where spin waves from the block AF phase, neutron spin resonance, and $(\pi, 0)$ excitations are marked as red solid circles, purple ellipses and light-blue cross shapes, respectively. (e) Integrated intensity comparison of several samples at $E = 14 \pm 2 \text{ meV}$. Olive Green: spin waves in the insulating $\text{Rb}_{0.89}\text{Fe}_{1.58}\text{Se}_2$; Dark red, light blue, and light violet are spin waves, $(\pi, 0)$ excitations, and resonance in SC $\text{Rb}_{0.82}\text{Fe}_{1.68}\text{Se}_2$; Orange: spin wave in BaFe_2As_2 . (f) Susceptibility measurement indicates $T_c = 32 \text{ K}$.

Results We have performed inelastic neutron scattering experiments on the ARCS chopper spectrometer at the Spallation Neutron Source, Oak Ridge National Laboratory using identical conditions as previous work on spin waves in insulating $\text{Rb}_{0.89}\text{Fe}_{1.58}\text{Se}_2$ [33]. Figures 1a and 1b show the $\sqrt{5} \times \sqrt{5}$ block AF structure and the positions of the AF peaks in reciprocal space, respectively [33]. We define the wave vector Q at (q_x, q_y, q_z) as $(H_o, K_o, L_o) = (q_x a_o/2\pi, q_y a_o/2\pi, q_z c_o/2\pi)$ rlu, where $a_o = 5.48$ and $c_o = 14.69 \text{ \AA}$ are the orthorhombic cell lattice parameters similar to iron pnictides [39]. In this notation, the neutron spin resonance [31, 32] occurs at $Q = (\pm 1, \pm 0.5)$ [or $Q = (\pm \pi, \pm 0.5\pi)$] (Fig. 1d), while the $\Gamma \leftrightarrow M$ Fermi surface nesting gives scattering at $Q = (\pm 1, 0)$ rlu (Figs. 1c and 1d). We co-aligned ~ 6 grams of the SC single crystals $\text{Rb}_{0.82}\text{Fe}_{1.68}\text{Se}_2$ grown by self-flux method (with mosaic of $\sim 6^\circ$) [33], where the chemical composition was determined by inductively-coupled plasma analysis. Figure 1f shows the temperature dependence of the susceptibility measurements confirming $T_c = 32 \text{ K}$. To ensure that the neutron spin resonance at $Q = (-1, 0.5)$ at $E = 14 \text{ meV}$ [31, 32] does not fall into detector gaps on ARCS, we rotated the co-aligned samples counter-clockwise by ~ 27 degrees. The incident beam energies were $E_i = 35, 80 \text{ meV}$ with E_i parallel to the c -axis. The scattering intensities were normalized to absolute units using a vanadium standard and can therefore be compared directly with spin waves in insulating $\text{Rb}_{0.89}\text{Fe}_{1.58}\text{Se}_2$ [33].

From earlier work on $A_y\text{Fe}_{1.6+x}\text{Se}_2$ [11–14], we know that superconductivity coexists with the block AF order. Therefore, one should expect acoustic spin waves in SC $\text{Rb}_{0.82}\text{Fe}_{1.68}\text{Se}_2$ from the block AF phase [33]. Figure 2 summarizes the two-dimensional constant-energy (E) images of spin excitations in the $[H_o, K_o]$ plane for insulating and SC $\text{Rb}_y\text{Fe}_{1.6+x}\text{Se}_2$. Since the subtle changes in the insulating and SC samples [11–14] are not expected to much affect phonons in these materials, we assume that the new dispersive features in $\text{Rb}_{0.82}\text{Fe}_{1.68}\text{Se}_2$ are spin excitations associated with the SC phase. Figures 2a-2d show images of acoustic spin waves at energies $E = 8 \pm 2, 12 \pm 2, 20 \pm 2,$ and $26 \pm 2 \text{ meV}$, respectively, for insulating $\text{Rb}_{0.89}\text{Fe}_{1.58}\text{Se}_2$ [33]. They are centered at the expected in-plane AF wave

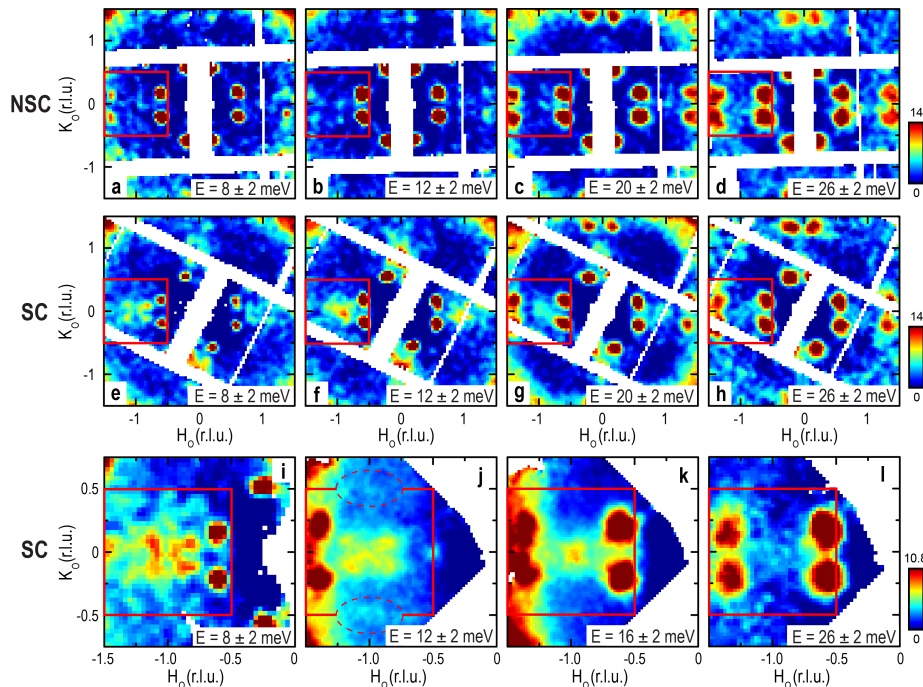


FIG. 2: (Color online) (a-d) Wave-vector dependence of spin-wave excitations at different energies for NSC $\text{Rb}_{0.89}\text{Fe}_{1.58}\text{Se}_2$ at 10 K obtained with incident neutron energy of $E_i = 80$ meV [33]. (e-h) Identical images for SC $\text{Rb}_{0.82}\text{Fe}_{1.68}\text{Se}_2$ at 6 K. The red squares are the Brillouin zone for iron pnictides [39]. (i-l) Expanded view of the excitations near $Q = (1, 0)$. The data in (j,k) are collected with $E_i = 35$ meV, while (i,l) are taken with $E_i = 80$ meV. The dashed ellipses in (j) mark positions of the resonance. The vertical color bars indicate intensity scale in mbarns/sr/meV/f.u.

vectors with no observable features at $Q = (1, \pm 0.5)$ and $Q = (1, 0)$ [33].

Figures 2e-2h plot images of the identical constant-energy cuts for SC $\text{Rb}_{0.82}\text{Fe}_{1.68}\text{Se}_2$ at $T = 6$ K. In addition to the usual spin waves from the block AF structure, we find new features near $Q = (\pm 1, 0)$ and $Q = (0, \pm 1)$. At $E = 8 \pm 2$ meV, there are four incommensurate peaks centered at $Q \approx (-1 \pm 0.14, \pm 0.1)$ (Fig. 2e). Upon increasing energies to $E = 12 \pm 2$ (Fig. 2f) and 20 ± 2 meV (Fig. 2g), the excitations become approximately centered at $Q = (\pm 1, 0)$. Finally at $E = 26 \pm 2$ meV, they disappear at $Q = (\pm 1, 0)$ and spin waves in SC $\text{Rb}_{0.82}\text{Fe}_{1.68}\text{Se}_2$ and insulating $\text{Rb}_{0.89}\text{Fe}_{1.58}\text{Se}_2$ become indistinguishable (Figs. 2d and 2h). Figures 2i-2l show the expanded view of the spin excitations near $Q = (-1, 0)$ at different energies. At $E = 8 \pm 2$ meV, we see four distinct peaks (Fig. 2i). At the neutron spin resonance energy of $E = 12 \pm 2$ meV, the excitations become cross-like near $Q = (-1, 0)$ and one can also see the resonance centered at $Q = (-1, \pm 0.5)$ (Fig. 2j) [31, 32]. Upon increasing energy to $E = 16 \pm 2$ meV, the excitations are well centered at $Q = (-1, 0)$ (Fig. 2k). Finally at $E = 26 \pm 2$ meV, we find only spin waves from the block AF phase centered around the expected AF positions.

To see how the excitations near $Q = (1, 0)$ respond to superconductivity and determine whether they are related to spin waves from the block AF phase, we show in Fig. 3 constant-energy cuts for the $Q = (1, 0)$ excitations and block AF spin waves at different temperatures. The neutron scattering cross section $S(Q, E)$ is related to the imaginary part of the dynamic susceptibility $\chi''(Q, \omega)$ by correcting for the Bose population factor via $S(Q, E) = 1/(1 - \exp(-E/(k_B T)))\chi''(Q, E)$, where k_B is the Boltzmann's constant. Figures 3a-3c show constant-energy cuts along the K_o direction for different temperatures at $E = 8 \pm 2$, 12 ± 2 , and 16 ± 2 meV, respectively. While $\chi''(Q, \omega)$ at the probed energies show no appreciable changes across T_c , it decreases on warming to $T = 250$ K, consistent with spin excitations. For comparison, we find that $\chi''(Q, \omega)$ of the spin waves from the block AF phase are temperature independent between 10 K and 250 K (Figs. 3d-3f). This is expected since spin waves are bosons and should follow the Bose factor below T_N . To see if superconductivity has any effect on spin waves of the block AF phase, we show in Figs. 3g-3i $\chi''(Q, \omega)$ for SC $\text{Rb}_{0.82}\text{Fe}_{1.68}\text{Se}_2$ and insulating $\text{Rb}_{0.89}\text{Fe}_{1.58}\text{Se}_2$. While the spin wave intensity at $E = 10 \pm 2$ and 20 ± 2 meV in the superconductor are lower than that of the insulator, it becomes similar at $E = 34 \pm 2$ meV. To quantitatively compare the differences between the intensity gain near $(-1, 0)$ with intensity loss of the AF spin waves in superconductor compared with that of the insulator, we plot in Fig. 3j the ratio of yellow area and yellow plus green areas for SC and insulating samples (Fig. 3k) as black square and yellow circles, respectively. We see that the

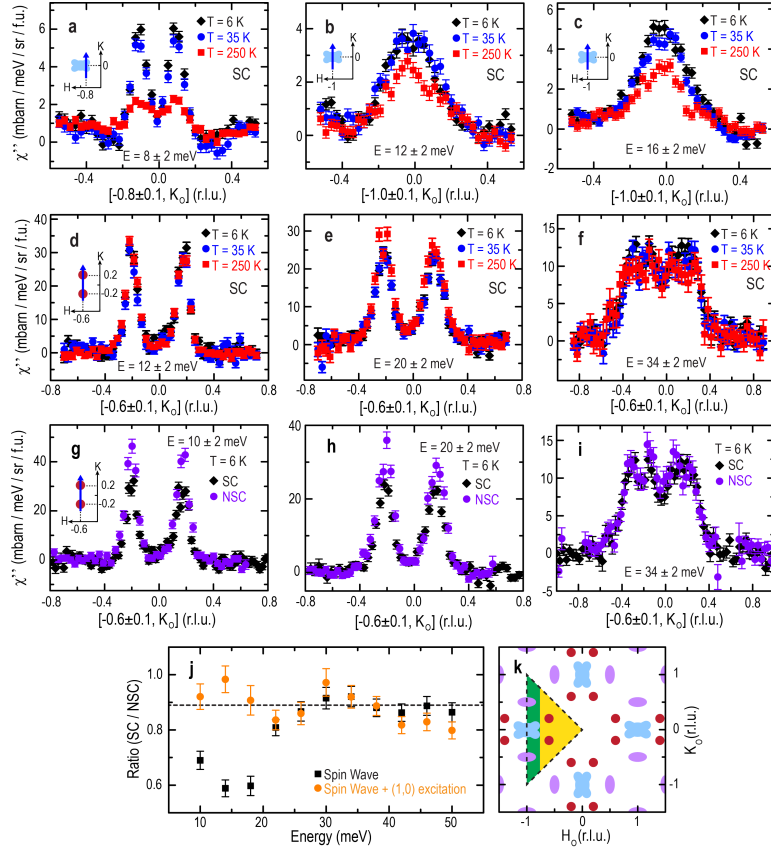


FIG. 3: Cuts of $\chi''(Q, \omega)$ along (a) the $[-0.8 \pm 0.1, K]$, (b,c) $[-1 \pm 0.1, K]$ directions for the $Q = (-1, 0)$ excitations at different temperatures. (d-f) Cuts of spin waves along the $[-0.6 \pm 0.1, K]$ direction at different energies and temperatures reveal that $\chi''(Q, \omega)$ is temperature independent up to $T = 250$ K. (g-i) Comparison of the low-temperature spin wave intensities for SC and insulating samples using the same cuts along the $[-0.6 \pm 0.1, K]$ direction. The spin wave intensity of the SC sample are lower at $E = 12 \pm 2$ and 20 ± 2 meV but become similar as that of the insulating sample at $E = 34 \pm 2$ meV. (j) The black squares are ratio of spin waves in yellow area for SC and insulating samples. The yellow circles are the ratio of excitations in yellow area + green area for SC and insulating samples. (k) Brillouin zone plot showing the shaded region.

spin wave intensity loss below ~ 30 meV is approximately compensated by an intensity gain from excitations around $(-1, 0)$.

Finally, to confirm the neutron spin resonance near $E = 14$ meV at $Q = (-1, 0.5)$ in our SC $\text{Rb}_{0.82}\text{Fe}_{1.68}\text{Se}_2$ [31, 32], we carried out constant- Q and constant-energy cuts to the data in Fig. 2j below and above T_c . Figure 4a shows the $S(Q, E)$ for integrated wave vectors $Q = (-0.5 \pm 0.1, 1 \pm 0.1)$ at 6 K and 35 K. The temperature difference plot (6 K–35 K) in Fig. 4b has a clear peak at $E = 14$ meV, thus confirming the neutron spin resonance in the SC state [31, 32]. Figures 2c and 2e show constant-energy cuts along the two different high symmetry directions (see insets) below and above T_c . The temperature difference plots show well-defined peaks at the expected wave vector, again consistent with previous work [31, 32]. Figure 1e compares the strength of the spin waves from the block AF structure in insulating and SC samples, the $(1, 0)$ spin excitations, the resonance, and spin waves of BaFe_2As_2 [39] near $E = 14$ meV.

Discussion The discovery of spin excitations near the $(\pi, 0)$ AF wave vector and their dispersion in SC $\text{Rb}_{0.82}\text{Fe}_{1.68}\text{Se}_2$ have several important implications. First, since ARPES experiments reveal that SC $A_y\text{Fe}_{1.6+x}\text{Se}_2$ have no hole-like Fermi surface at $\Gamma(0, 0)$ [5–7], the $(\pi, 0)$ spin excitations cannot arise from quasiparticle excitations between Γ and M points and most likely come from localized magnetic moments [34]. Taking into account that SC $\text{Rb}_{0.82}\text{Fe}_{1.68}\text{Se}_2$ also has a neutron spin resonance most likely arising from Fermi surface nesting and itinerant electrons [31, 32], these results suggest that localized moments and itinerant electrons are both important ingredients for magnetism in alkaline iron selenide superconductors. Second, the observation of low-energy incommensurate spin excitations and its inverse dispersion are reminiscent of the spin excitations for copper oxide superconductors [35, 36] and insulating $\text{La}_{2-x}\text{Sr}_x\text{CoO}_4$ [37]. This suggests that the $(\pi, 0)$ spin excitations stem from strongly correlated elec-

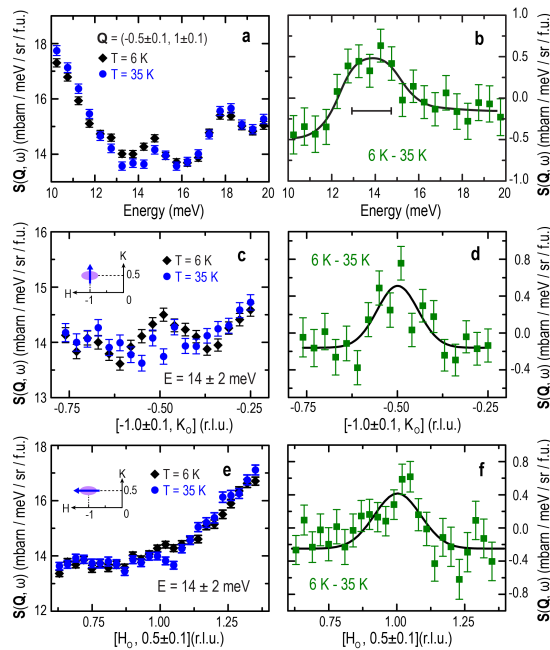


FIG. 4: (a) Energy cut at the resonance position by integrating $Q = (-0.5 \pm 0.1, 1 \pm 0.1)$. (b) Subtracting 35 K data from 6 K data shows a resonance at $E = 14$ meV. The horizontal bar is the instrumental energy resolution. Constant-energy cuts along the (c) $[H, 1 \pm 0.1]$ and (e) $[0.5 \pm 0.1, K]$ directions. The 6 K–35 K data confirm the resonance peak at $(1, -0.5)$ with a width $FWHM = 0.13 \pm 0.04$ along the H direction and $FWHM = 0.20 \pm 0.05$ along the K direction.

tronic physics and may be associated with dynamic stripes [38]. Third, the reduction in the low-energy spin wave intensity for the block AF phase in SC $\text{Rb}_{0.82}\text{Fe}_{1.68}\text{Se}_2$ and the concurrent appearance of the incommensurate spin excitations near $Q = (\pi, 0)$ indicate that spin excitations in superconductors are compensated by spin waves in the AF block phase. If the SC phase in $\text{Rb}_{0.82}\text{Fe}_{1.68}\text{Se}_2$ mesoscopically coexists with the block AF phase [16–23], one can imagine the formation of a striped phase on the interface region of the block AF phase and the SC phase due to the interaction between local moments and itinerant electrons. The latter can be viewed as dopants to a Mott insulator phase and naturally result in a stripe phase as in the case of copper oxides [38].

Acknowledgements We thank Qimiao Si for helpful discussions and R. Zhang for work at IOP. The work at UTK is supported by the U.S. NSF-DMR-1063866 and NSF-OISE-0968226. Work at IOP is supported by the MOST of China 973 program (2012CB821400) and by NSFC-51002180. ORNL neutron scattering facilities are supported by the U.S. DOE, Division of Scientific User Facilities.

* Electronic address: pdai@utk.edu

- [1] J. G. Guo *et al.*, Phys. Rev. B **82**, 180520(R) (2010).
- [2] A. Krzton-Maziopa, A. *et al.*, J. Phys.: Condens. Matter **23**, 052203 (2011).
- [3] M. H. Fang *et al.*, EuroPhys. Lett., **94**, 27009 (2011).
- [4] A. F. Wang *et al.*, Phys. Rev. B **83**, 060512 (2011).
- [5] Y. Zhang *et al.*, Nature Materials **10**, 273-277 (2011).
- [6] T. Qian *et al.*, Phys. Rev. Lett. **106**, 187001 (2011).
- [7] D. X. Mou *et al.*, Phys. Rev. Lett. **106**, 107001 (2011).
- [8] I. I. Mazin, Nature (London) **464**, 183 (2010).
- [9] D. C. Johnston, Adv. in Phys. **59**, 803 (2010).
- [10] L. Häggström, A. Seidel, and R. Berger, J. Magn. Magn. Mater. **98**, 37 (1991).
- [11] W. Bao *et al.*, Chinese Phys. Lett. **28**, 086104 (2011).
- [12] V. Yu *et al.*, Phys. Rev. B **83**, 144410 (2011).
- [13] F. Ye *et al.*, Phys. Rev. Lett. **107**, 137003 (2011).
- [14] M. Wang *et al.*, Phys. Rev. B **84**, 094504 (2011).

- [15] C. de la Cruz *et al.*, Nature (London) **453**, 899-902 (2008).
- [16] Y. J. Song, Z. Wang, Z.W. Wang, H. L. Shi, Z. Chen, H. F. Tian, G. F. Chen, H. X. Yang, and J. Q. Li, Europhys. Lett. **95**, 37007 (2011).
- [17] A. Ricci *et al.*, Phys. Rev. B **84**, 060511 (2011).
- [18] Z. Shermanini *et al.*, arXiv:1111.5142.
- [19] W. Li *et al.*, Nature Physics: doi:10.1038/nphys2155.
- [20] F. Chen *et al.*, Phys. Rev. X **1**, 021020 (2011).
- [21] V. Ksenofontov, G. Wortmann, S. A. Medvedev, V. Tsurkan, J. Deisenhofer, A. Loidl, and C. Felser, Phys. Rev. B **84**, 180508(R) (2011).
- [22] A. Charnukha *et al.*, arXiv:1108.5698v1.
- [23] C. C. Homes, Z. J. Xu, J. S. Wen, and G. D. Gu, arXiv:1110.5529v1.
- [24] T. A. Maier and D. J. Scalapino, Phys. Rev. B **78**, 020514(R) (2008).
- [25] M. M. Korshunov and I. Eremin, Phys. Rev. B **78**, 140509(R) (2008).
- [26] M. D. Lumsden *et al.* Phys. Rev. Lett. **102**, 107005 (2009).
- [27] S. Chi *et al.*, Phys. Rev. Lett. **102**, 107006 (2009).
- [28] D. S. Inosov *et al.*, Nature Phys. **6**, 178 (2010).
- [29] C. L. Zhang *et al.*, Scientific Reports **1**, 115 (2011).
- [30] T. A. Maier, S. Graser, P. J. Hirschfeld, and D. J. Scalapino, Phys. Rev. B **83**, 100515(R) (2011).
- [31] G. Friemel *et al.*, arXiv:1112.1636v1.
- [32] J. T. Park *et al.*, Phys. Rev. Lett. **107**, 177005 (2011).
- [33] M. Y. Wang *et al.*, Nature Commun. **2**, 580 (2011).
- [34] Q. Si and E. Abrahams, Phys. Rev. Lett. **101**, 76401 (2008).
- [35] S. M. Hayden, H. A. Mook, P. Dai, T. G. Perring, and F. Doğan, Nature **429**, 531 (2004).
- [36] J. M. Tranquada, H. Woo, T. G. Perring, H. Goka, G. D. Gu, G. Xu, M. Fujita, and K. Yamada, Nature **429**, 534 (2004).
- [37] A. T. Boothroyd, P. Babkevich, D. Prabhakaran, and P. G. Freeman, Nature (London) **471**, 341 (2011).
- [38] S. A. Kivelson *et al.*, Rev. Mod. Phys. **75**, 1201 (2003).
- [39] L. W. Harriger, H. Q. Luo, M. S. Liu, C. Frost, J. P. Hu, M. R. Norman, and P. Dai, Phys. Rev. B **84**, 054544 (2011).